

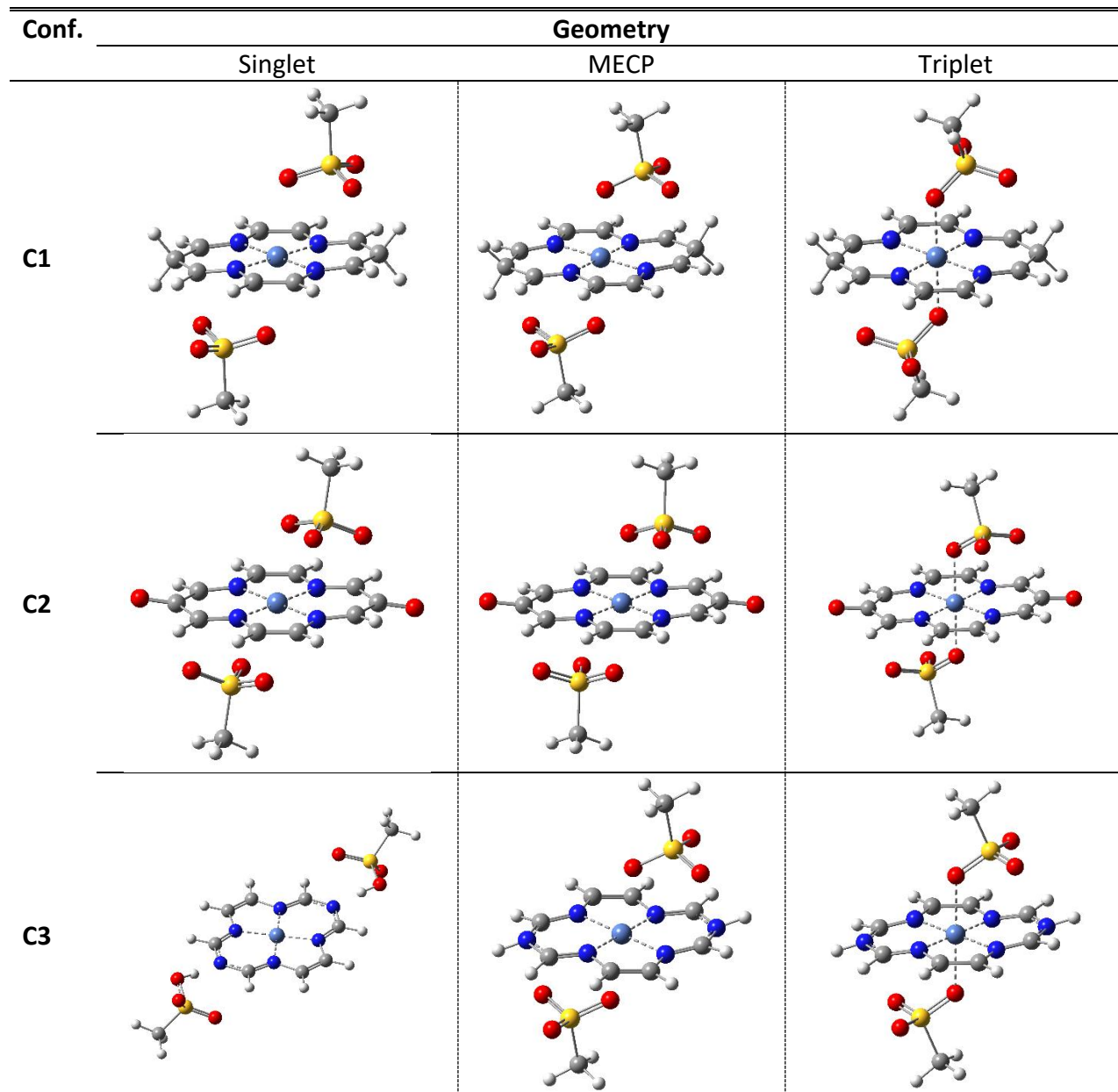
Supporting Material

Improving the light-induced spin transition efficiency in Ni(II)-based macrocyclic-ligand complexes

Alex A. Farcaș^{a,b} and Attila Bende*,^a

^aNational Institute for Research and Development of Isotopic and Molecular Technologies, Donat Street, No. 67-103, Ro-400293, Cluj-Napoca, Romania.

^bFaculty of Physics, "Babeş-Bolyai" University, Mihail Kogalniceanu Street No. 1, Ro-400084 Cluj-Napoca, Romania.



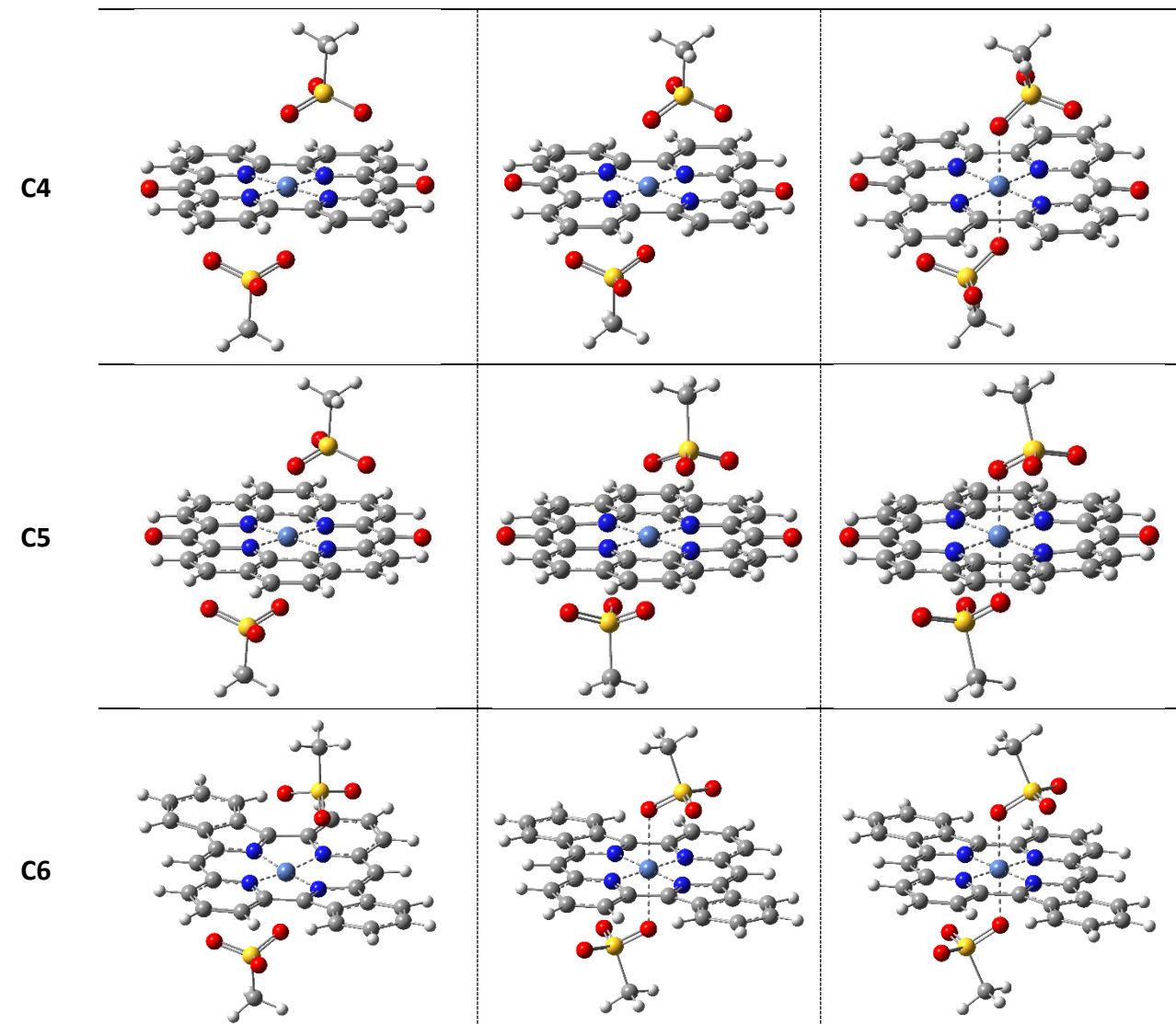


Figure S1. The equilibrium geometry conformation of the six proposed C1-C6 organometallic complexes for the singlet and triplet spin configurations as well as for the minimum energy crossing point (MECP) geometries of the ground state singlet and triplet energies calculated at M06/def2-TZVP level of theory.

Table S1. The singlet-triplet energy gap (in eV) for the C4 organometallic complex obtained with six different exchange-correlation functionals (M06L [1], revM06L [2], B3LYP* [3], B3LYP*-D3 [3-5], M06 [6] and MN12-SX [7]) implemented in the ORCA program package [8,9] and considering the Def2-TZVP basis set [10].

Geom.	XC Functionals					
	M06L	revM06L	B3LYP*	B3LYP*-D3	M06	MN12-SX*
Singlet	0.668	0.587	0.595	0.592	0.448	0.378
MECP	0.722	0.690	0.614	0.606	0.642	N/A
Triplet	0.000	0.000	0.000	0.000	0.000	0.000

*The MN12-SX results were obtained using the GAUSSIAN09 software package [11].

Table S2. The characteristic ligand bond distances (in Å) between the Ni(II) central atom and the oxygen or nitrogen atoms for singlet and triplet spin configurations as well as for the minimum energy crossing point (MECP) geometries of the ground state singlet and triplet energies of the C4 metal-organic complex obtained at M06/CPCM/def2-TZVP level of theory considering two different solvents. The relative conformational energies (E^{conf} in eV) between singlet, triplet, and MECP geometries are also given in the last column.

Solv.	Geom.	$O_{\perp}\cdots Ni$ (Å)	$N_{ }\cdots Ni$ (Å)	E^{conf} (eV)
Vacuum	Sing.	2.573	1.921, 1.921	0.448
		2.566	1.915, 1.915	
	MECP	2.439	1.937, 1.937	0.642
		2.438	1.940, 1.940	
	Trip.	2.130	1.997, 1.997	0.000
		2.130	2.001, 2.001	
Chloroform	Sing.	2.689	1.912, 1.912	0.380
		2.692	1.913, 1.913	
	MECP	2.499	1.934, 1.934	0.434
		2.499	1.936, 1.936	
	Trip.	2.159	1.993, 1.993	0.000
		2.159	1.994, 1.994	
DMSO	Sing.	2.707	1.911, 1.911	0.305
		2.714	1.912, 1.912	
	MECP	2.403	1.929, 1.929	0.527
		2.403	1.931, 1.931	
	Trip.	2.165	1.991, 1.992	0.000
		2.166	1.993, 1.993	

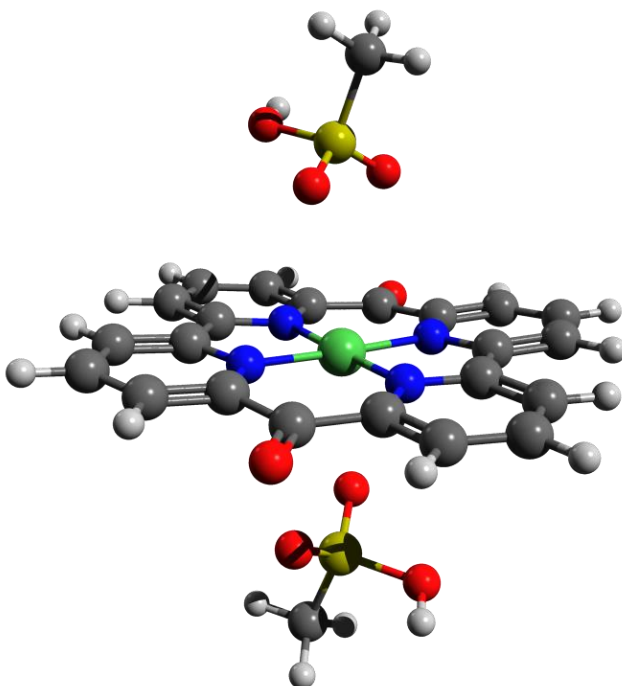
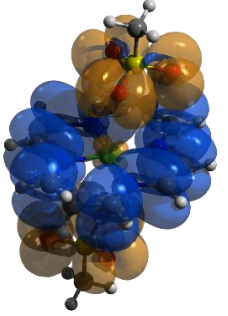
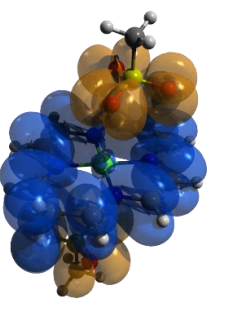
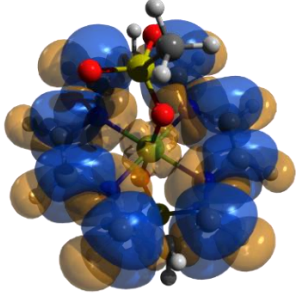
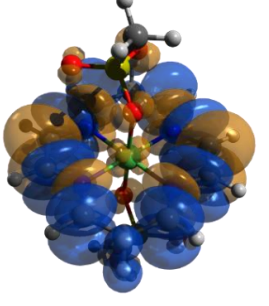
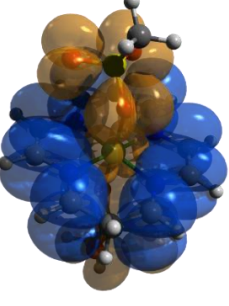
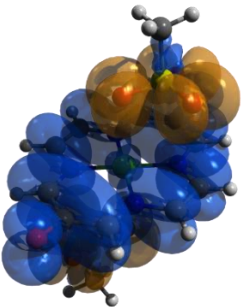
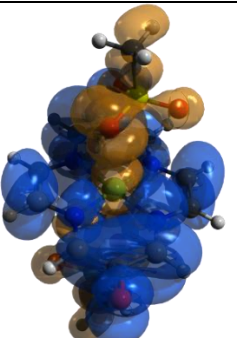
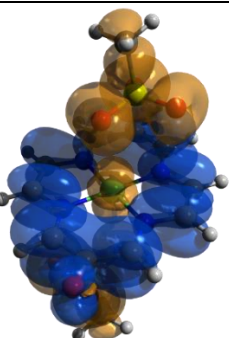
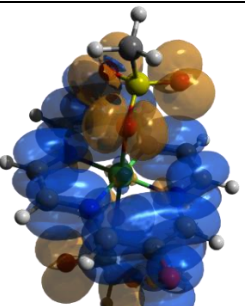
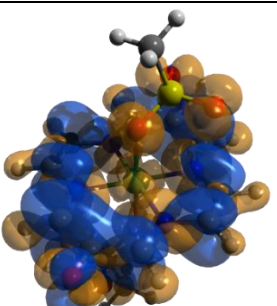
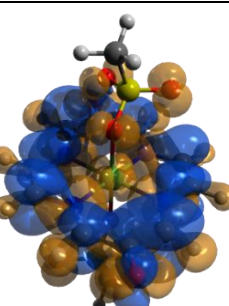


Figure S2. The geometry configuration of the complex built by the Ni(II)–diketo-porphyrin and two neutral mesylate groups computed for the singlet spin state at M06/def2-tzvp level of theory.

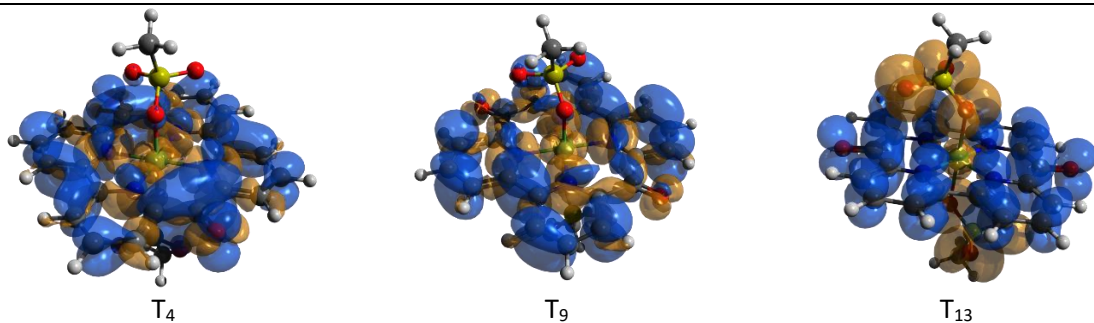
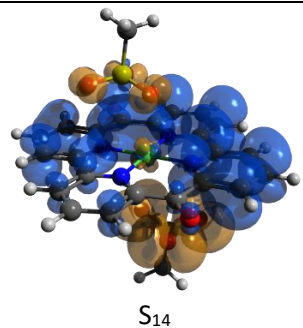
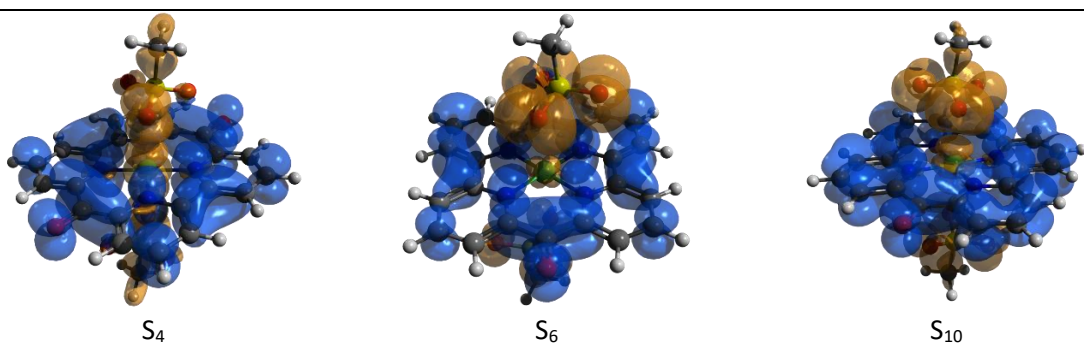
Table S3. The fractional electron population of different fragments (Ni(II), PL – planar ligand, VL – vertical ligand), the natural electron population of the central Ni cation, as well as the natural electron population of the 3d orbitals of the central Ni cation for the C4-C6 organometallic complexes, obtained at NBO/M06/def2-TZVP level of theory.

Natural Population of the metal ion and ligand fragments					
Struct.	POP ^{Ni(II)}	POP ^{PL}	POP ^{VL}	CT PL→Ni(II)	CT VL→Ni(II)
C4 ^S	+0.61e	+1.13e	-0.87e -0.87e	-1.13e	-0.13e -0.13e
C4 ^T	+0.81e	+0.74e	-0.78e -0.78e	-0.74e	-0.22e -0.22e
C5 ^S	+0.61e	+1.13e	-0.87e -0.87e	-1.13e	-0.13e -0.13e
C5 ^T	+0.80e	+0.75e	-0.77e -0.77e	-0.75e	-0.23e -0.23e
C6 ^S	+0.54e	+1.25e	-0.87e -0.92e	-1.25e	-0.13e -0.08e
C6 ^T	+0.66e	+0.81e	-0.74e -0.74e	-0.81e	-0.26e -0.26e
Ni electron population					
C4 ^S	Ar4s[0.26]3d[8.66]4p[0.45]4d[0.02]				
C4 ^T	Ar4s[α:0.12,β:0.12]3d[α:4.95,β:3.41]4p[α:0.27,β:0.28]4d[α:0.02,β:0.01]				
C5 ^S	Ar4s[0.26]3d[8.68]4p[0.44]4d[0.02]				
C5 ^T	Ar4s[α:0.12,β:0.12]3d[α:4.95,β:3.42]4p[α:0.27,β:0.29]4d[α: 0.02,β:0.01]				
C6 ^S	Ar4s[0.27]3d[8.69]4p[0.48]4d[0.02]				
C6 ^T	Ar4s[α:0.13,β:0.13]3d[α:4.55,β:3.82]4p[α:0.33,β:0.34]4d[α:0.02,β:0.01]				
Ni 3d orbital population					
	d _{xy}	d _{xz}	d _{yz}	d _{x²-y²}	d _{z²}
C4 ^S	1.50	1.85	1.85	1.57	1.92
C4 ^T	1.79 α:0.99,β:0.80	1.48 α:0.99,β:0.49	1.92 α:0.98,β:0.94	1.57 α:0.99,β:0.58	1.59 α:0.99,β:0.60
C5 ^S	1.65	1.68	1.94	1.44	1.96
C5 ^T	1.55 α:0.99,β:0.56	1.65 α:0.99,β:0.66	1.78 α:0.99,β:0.77	1.81 α:0.99,β:0.82	1.59 α:0.99,β:0.60
C6 ^S	1.93	1.87	1.76	1.29	1.84
C6 ^T	1.95 α:0.98,β:0.97	1.91 α:0.96,β:0.95	1.45 α:0.94,β:0.51	1.34 α:0.70,β:0.64	1.71 α:0.96,β:0.75

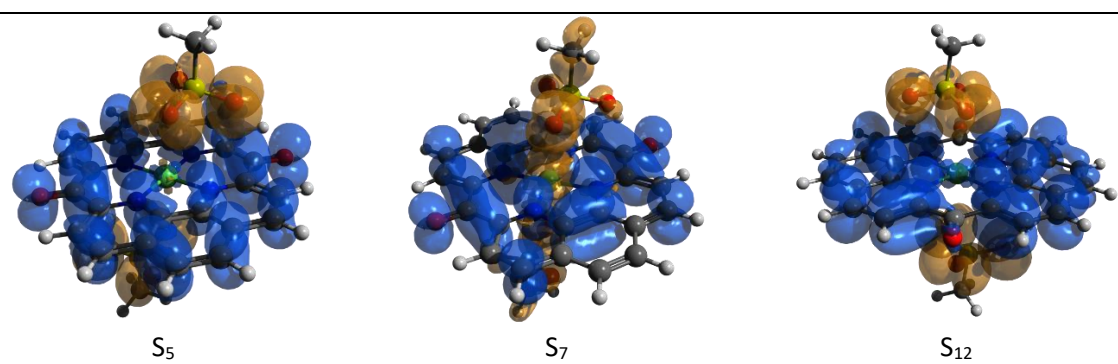
Table S4. The orbital shapes of the Natural Difference Orbitals (NDO) obtained as the difference between the corresponding ground state and the electronic excited state densities for the five (C1, C2, C4-C6) organometallic complexes with octahedral coordination computed at TD-DFT/M06/Def2-TZVP level of theory (blue is the positive and orange means the negative densities).

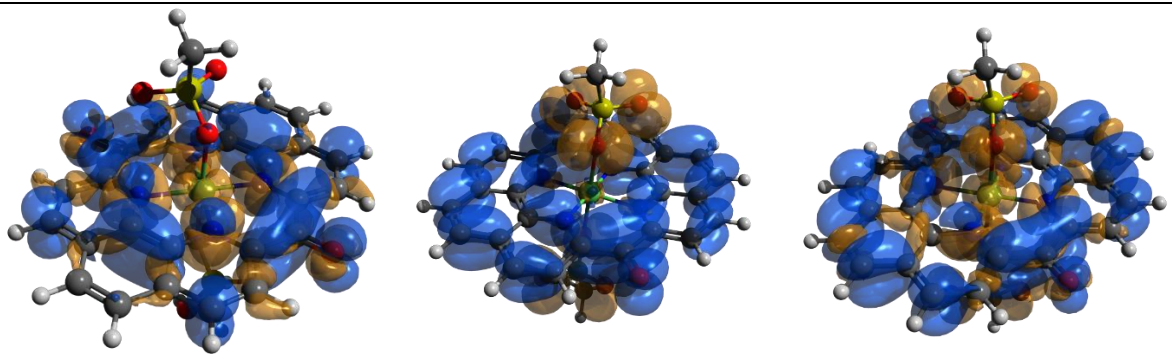
Struct.	Natural Difference Orbitals		
C1			
			
C2			
			

C4



C5



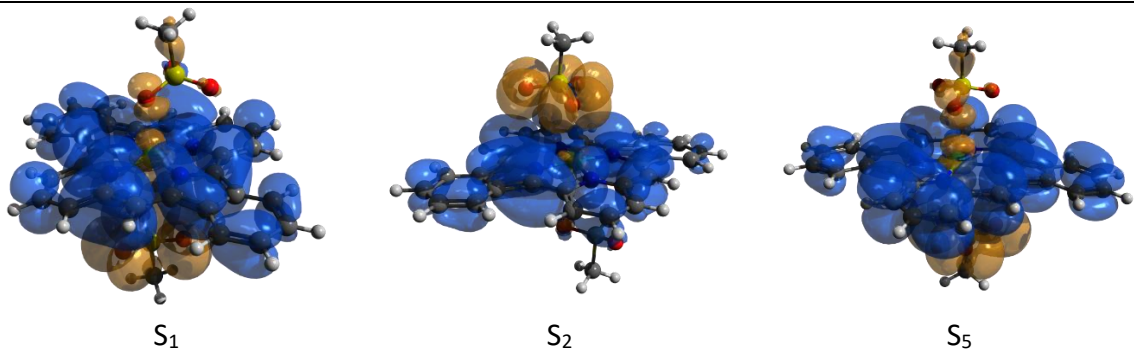


T_6

T_{12}

T_{14}

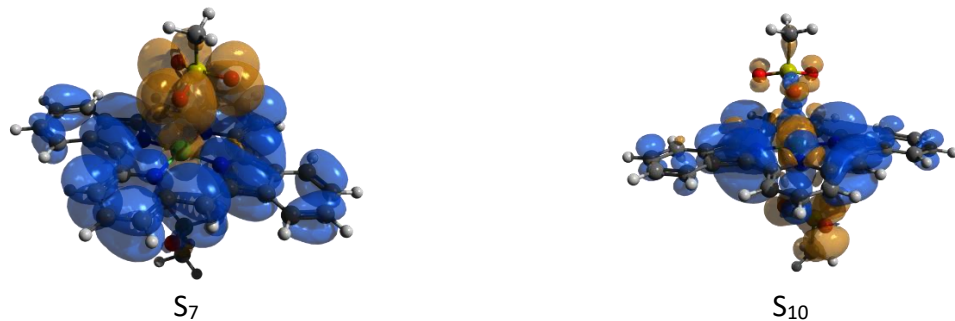
C6



S_1

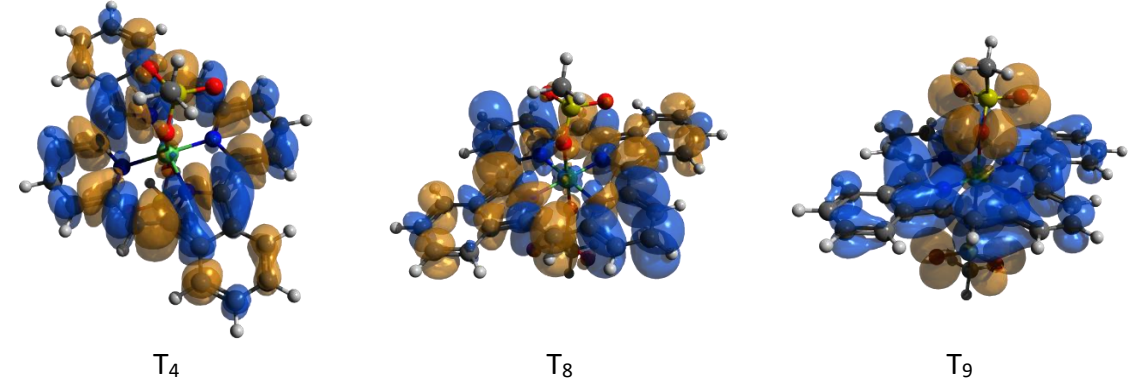
S_2

S_5



S_7

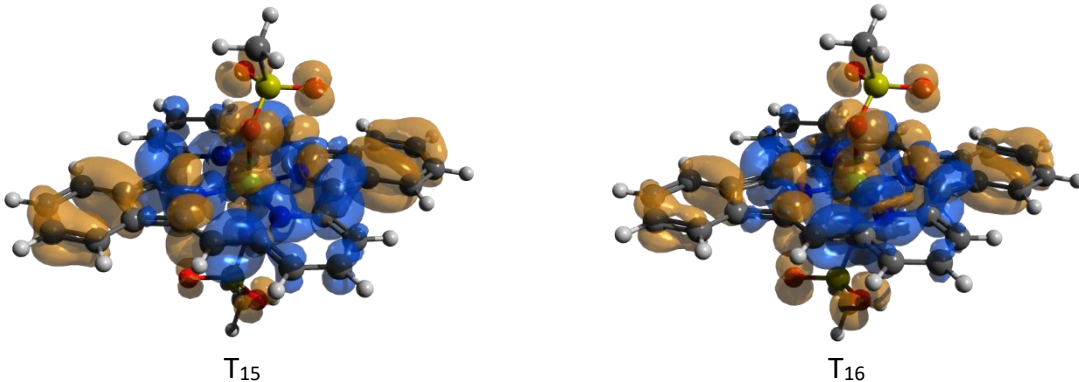
S_{10}



T_4

T_8

T_9



References

- Zhao, Y.; Truhlar, D.G. A new local density functional for main-group thermochemistry, transition metal bonding, thermochemical kinetics, and noncovalent interactions. *J. Chem. Phys.* **2006**, *125*(19), [194101](#).
- Wang, Y.; Jin, X.; Yu, H.S.; Truhlar, D.G.; Hea, X. Revised M06-L functional for improved accuracy on chemical reaction barrier heights, noncovalent interactions, and solid-state physics. *Proc. Natl. Acad. Sci. USA* **2017**, *114*(32), [8487–8492](#).
- Salomon, O.; Reiher, M.; Hess, B. Assertion and validation of the performance of the B3LYP* functional for the first transition metal row and the G2 test set. *J. Chem. Phys.* **2002**, *117*(10), [4729–4737](#).
- Grimme, S.; Antony, J.; Ehrlich, S.; Krieg, S. A consistent and accurate ab initio parametrization of density functional dispersion correction (DFT-D) for the 94 elements H-Pu. *J. Chem. Phys.* **2010**, *132*, [154104](#).
- Grimme, S.; Ehrlich, S.; Goerigk, L. Effect of the damping function in dispersion corrected density functional theory, *J. Comp. Chem.* **2011**, *32*(7), [1456–1465](#).
- Zhao, Y.; Truhlar, D. The M06 suite of density functionals for main group thermochemistry, thermochemical kinetics, noncovalent interactions, excited states, and transition elements: two new functionals and systematic testing of four M06-class functionals and 12 other functionals. *Theor. Chem. Acc.* **2008**, *120*, [215–241](#).
- Peverati, R.; Truhlar, D.G. Screened-exchange density functionals with broad accuracy for chemistry and solid-state physics. *Phys. Chem. Chem. Phys.* **2012**, *14*(47): [16187–16191](#).
- Neese, F. The ORCA program system. *Wires Comput. Mol. Sci.* **2012**, *2*, [73–78](#).
- Neese, F. Software update: the ORCA program system, version 4.0. *Wires Comput. Mol. Sci.* **2018**, *8*, [e1327](#).
- Weigend, F.; Ahlrichs, R. Balanced basis sets of split valence, triple zeta valence and quadruple zeta valence quality for H to Rn: Design and assessment of accuracy. *Phys. Chem. Chem. Phys.* **2005**, *7*, [3297–3305](#).
- GAUSSIAN09, Revision D.01, M. J. Frisch, G. W. Trucks, H. B. Schlegel, G. E. Scuseria, M. A. Robb et al. Gaussian, Inc., Wallingford CT, 2013.